Bioorg. Med. Chem. 29 (2021) 115881

Contents lists available at ScienceDirect

Bioorganic & Medicinal Chemistry

journal homepage: www.elsevier.com/locate/bmc

Fluorescent molecular rotors as sensors for the detection of thymidine phosphorylase

Manuela Petaccia [a,c], Luisa Giansanti [a,c,*], James N. Wilson [b], Heajin Lee [b,1], Sara Battista [a], Giovanna Mancini [c]

[a] Dipartimento di Scienze Fisiche e Chimiche, Università degli Studi dell'Aquila, Via Vetoio 10, 67100 Coppito (Aq), Italy
[b] Department of Chemistry, University of Miami, 1301 Memorial Drive, Coral Gables, FL 33124, USA
[c] CNR – Istituto per i Sistemi Biologici, Via Salaria km 29.300, 00016 Monterotondo Scalo (RM), Italy

ARTICLE INFO

Keywords:
Molecular Rotor
Thymidine Phosphorylase
5-Fluoruracil
Fluorescent Sensor
Spacer Length

ABSTRACT

Three new fluorescent molecular rotors were synthesized with the aim of using them as sensors to dose thymidine phosphorylase, one of the target enzymes of 5-fluorouracil, a potent chemotherapic drug largely used in the treatment of many solid tumors, that acts by hindering the metabolism of pyrimidines. 5-Fluorouracil has a very narrow therapeutic window, in fact, its optimal dosage is strictly related to the level of its target enzymes that vary significantly among patients, and it would be of the utmost importance to have an easy and fast method to detect and quantify them.

The three molecular rotors developed as TP sensors differ in the length of the alkylic spacer joining the ligand unit, a thymine moiety, and the fluorescent molecular rotor, a [4-(1-dimethylamino)phenyl]-pyridinium bromide. Their ability to trigger an optical signal upon the interaction with thymidine phosphorylase was investigated by fluorescent measurements.

1. Introduction

Thymidine phosphorylase, TP, thymidylate synthase and dihydropyrimidine dehydrogenase, DPD, are the target enzymes of 5–fluorouracil (5-FU), a chemotherapeutic agent that interferes with the metabolism of pyrimidines and that is used in the treatment of many solid malignant tumors (breast, colon, and skin cancer). 5-FU has a very narrow therapeutic window and only approximately 25% of patients are treated with the optimal dose of it, whereas in the other cases patients are overdosed or underdosed with a consequent increase of the toxic side effects or a reduction of the therapeutic efficacy, respectively.[1,2] The high variability of the efficacy of the treatment is strictly related to the variability of the level of the target enzymes of 5-FU in patients tissues.[3–5] In addition, 5–8% of patients are affected by DPD deficiency[6] and for them the administration of the drug can be fatal because DPD is directly involved in 5-FU catabolism. At present 5-FU is typically dosed after evaluating body surface area of each, but it is well known that this estimation bring to different 5-FU systemic exposure for patient because levels of 5-FU in plasma can significantly vary also between subjects with similar body surface area.[7,8] It is thus evident that a reliable, and possibly inexpensive, method to rapidly and easily detect the presence of these enzymes in patients before and during the treatment with 5-FU is a serious medical issue.

In general, a chemical sensor requires the assembly of one or more receptor units together with a transducer part in a defined geometry to allow the fast and reliable identification of the presence or the absence of specific target molecules. Usually the sensing element and the transducer are distinct components packaged together in direct spatial contact in the same unit. In certain chemical sensors the sensing element and the transducer responsible of signaling the recognition event are parts of the same molecule,[9] so they are in close proximity because covalently linked though electronically independent[10–12] When the response signal is based on fluorescence these sensors are called extrinsic fluorescent probes or conjugates[13] with the interaction of the analyte with the receptor inducing a change in the fluorophore surroundings and, as a consequence, in its emission.

We previously described a fluorescent sensor for the detection of TP based on liposomes containing both an amphiphile tail-tagged with a

* Corresponding author.
E-mail address: luisa.giansanti@univaq.it (L. Giansanti).
[1] Present address: Department of Chemistry, Tampa University, 401 W. Kennedy Blvd. Tampa, FL 33606.

https://doi.org/10.1016/j.bmc.2020.115881
Received 9 October 2020; Received in revised form 12 November 2020; Accepted 13 November 2020
Available online 21 November 2020

pyrene moiety and a 5-FU derivative, where the fluorescence signal occurred upon the interaction of 5-FU derivative with TP, due to the variation of excimer/monomer ratio of pyrene residues.[14] In that case the sensor elements were not covalently linked. Here we report the synthesis and the characterization of new extrinsic fluorescent molecular probes (**1**, **2** and **3**, Chart 2) designed to detect the target enzymes of 5-FU. The evaluation of binding and sensor capabilities was carried out on TP because it is the only commercially available among the three target enzymes.

The three newly synthesized fluorescent molecules differ for the length of the alkyl spacer joining the receptor unit, a thymine moiety, and the fluorophore residue responsible of signaling the recognition event, a [4-(1-dimethylamino)phenyl]-pyridinium bromide, a molecular rotor (MR). Among MRs, the fluorescence properties of *p*-(dimethylamino)-benzene derivatives have been extensively studied.[15–18] The probes **1**, **2** and **3**, belonging to this class of MRs, exhibit the so-called "turn-on" emission as a function of their chemical microenvironment. The presence of the electron donating dimethyl amino group coupled opposite to the electron withdrawing *N*-methylpyridinium ring yields a molecule with strong charge transfer character in the planar locally excited (LE) state. Another feature that contributes to the high sensitivity of these compounds is the ability of the molecule to twist from coplanarity, that is, to form a dihedral angle φ between the aniline and pyridinium rings (Figure 1) significantly different from zero.

The minimum excited-state energy is reached when the aniline (donor) and pyridinium ring (acceptor) planes are rotated 90° relative to each other (Figure 1). In this geometrical condition the energy gap between the twisted intramolecular charge transfer (TICT) state and the ground state (GS) becomes dramatically small and the relaxation from this twisted state is practically radiationless.[17,19] Polar solvents conceivably help to stabilize the TICT state resulting in a shift to lower emission energies as well as lead to emission quenching. On the other hand, apolar solvents do not particularly favor the formation of TICT state with consequent increase of emission intensity.[18] The twisting is also supposed to be limited in viscous solvents or in geometrically confined environments hence resulting in a sharp increase of emission.[20] The binding of the new fluorescent molecules with the binding site of the target enzymes, promoted by the presence of thymine, should place the MR in a less polar and restrictive environment compared to the free molecule in aqueous solvent. In this configuration turn-on emission of the MR should occur. This approach offers the advantage of minimizing background emission from unbound MR, because the emission in aqueous solvent is turned-off.

The different length of the alkylic spacer of the three new fluorescent MRs **1**–**3** might affect the ability to show the turn-on emission upon the binding with TP because the fluorophore should be located in environments characterized by different local polarity and/or steric hindrance as a function of the aminoacidic composition of the enzymatic pocket and of its conformation. The ability of the three MRs to trigger an optical signal upon the interaction with the target enzyme was investigated by fluorescent measurements.

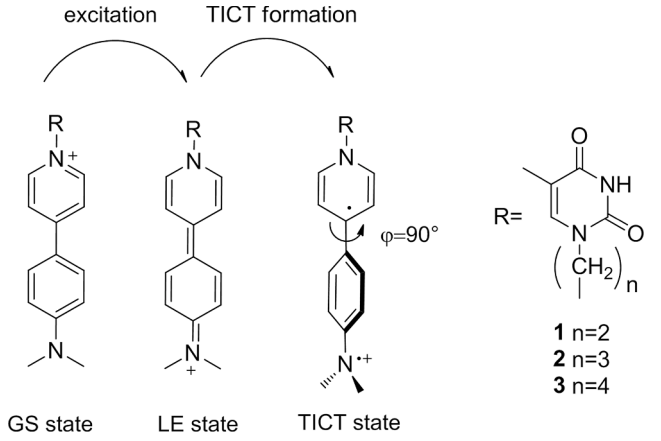

Fig. 1. Intramolecular twisting of MR of **1**, **2** and **3**.

2. Experimental section

2.1. Instrumentation

^{1}H and ^{13}C NMR spectra were carried out on a Varian NMR 500 MHz; δ in ppm relative to the residual solvent peak of $CDCl_3$ at 7.26 and 77.0 ppm for 1H and 13C, respectively; J in Hz.

Steady-state fluorescence experiments were carried out on a Fluoromax-4 Horiba-Jobin Yvon spectrofluorimeter.

High-resolution electrospray ionisation mass spectrometry (HRESIMS) spectra were recorded using a Micromass Q-TOF Micromass spectrometer (Waters) in the electrospray-ionization mode.

2.2. Materials

Phosphate–buffered saline (PBS, 0.01 M phosphate buffer; 0.0027 M KCl; 0.137 M NaCl; pH 7.4), TP recombinant from *Escherichia coli* and all reagents employed for the synthesis of **1**–**3** were purchased from Sigma-Aldrich and were used without further purification.

2.2.1. Synthesis of pyrimidines 1b, 2b and 3b

α,ω-Alkyldibromide 1a (**2a**, **3a**) (1 eq) was added to a solution of thymine (4 eq) dissolved in DMF ("purum" grade bottle) (26 eq) followed by anhydrous potassium carbonate (2 eq). The mixture was stirred for 48 h at room temperature. The resulting slurry was filtered through a Celite pad and the cake washed two times with DMF (5 mL). The solvent was removed under reduced pressure to give **1b** (**2b, 3b**) as a white solid that was purified by column chromatography on silica gel using CH_2C1_2/ETOAc 9:1 as eluent (yield 37% for **1b**, 45% for **2b** and 55% for **3b**). Compound **1b:** ^{1}H NMR ($CDCl_3$) δ ppm 1.86 (d, 3H, $J = 1.5$ Hz), 2.51 (t, 3H, $J = 2$ Hz), 4.16 (t, $J = 8$ Hz, 2H), 4.67 (t, $J = 8$ Hz, 2H), 7.57 (d, $J = 1$ Hz, 1H) ^{13}C NMR (500 MHz, CDCI3) 8 12.44, 42.45, 66.17, 116.93, 151.01, 158.43, 161.55. Compound **2b:** ^{1}H NMR ($CDCl_3$) δ ppm 1.31 (m, J = 1.2, 4H), 2.05 (s, 3H), 3.44 (t, $J = 8.5$ Hz, 2H), 3.88 (t, $J = 8.5$ Hz, 2H), 7.53 (s, 1H), 11.2 (s, 1H). ^{13}C NMR (500 MHz, CDCI3) δ ppm 12.4, 30.1, 35.9, 48.9, 110.9, 139.2, 150.8, 163.7. Compound **3b:** ^{1}H NMR ($CDCl_3$) δ ppm 1.67–1.71 (m, 3H, $J = 6$ Hz), 1.74–1.79 (m, 3H, $J = 6$ Hz), 2.50 (s, 3H) 3.55 (t, $J = 6.5$ Hz, 2H), 3.65 (t, $J = 6.5$ Hz, 2H), 7.54 (s, 1H), 11.23 (s, 1H). ^{13}C NMR ($CDCl_3$) δ ppm 12.43, 27.67, 29.64, 34.98, 46.73, 109, 141.81, 151.37, 164.74.

2.2.2. Synthesis of 4-[4-(1-Dimethylamino)phenyl]-pyridine (DMAPP)

Palladium (II) acetate (5% mol) and triphenylphosphine (10% mol) were added to a mixture of 4-bromopyridine HCl (1.2 eq), then a solution of 4-(dimethylamino)phenylboronic (1 eq), and potassium carbonate (3 eq) in dimethylformamide (DMF, 1.5 mL) was added. The reaction mixture was kept at reflux overnight, then filtered through a celite plug and concentrated. The crude product was purified by flash chromatography (silica, CH_2Cl_2/ETOAc = 99:1 → 95:5) to give the product, DMAPP, as a tan solid (30%). ^{1}H NMR ($CDCl_3$): δ ppm 8.56 (d, $J = 4.9$ Hz, 2H), 7.61 – 7.55 (m, 2H), 7.46 (dd, $J = 4.7$, 1.5 Hz, 2H), 6.82 – 6.76 (m, 2H), 3.02 (s, 6H) ^{13}C NMR ($CDCl_3$): δ ppm 41.3, 112.7, 120.6, 128.3, 131.2, 147.2, 149.7, 155.8.

2.2.3. Synthesis of MRs *1*, *2* and *3*

4-[4-(1-Dimethylamino)phenyl]-pyridine (1 eq) was combined with 1 eq of 1b (2b, 3b) and 0.5–4.0 mL of DMF. The reaction mixture was heated at 80 °C for 48 h to observe the formation of a yellow precipitate. After cooling the reaction mixture, the crude product was isolated by suction filtration and rinsed with EtOAc. The crude product was crystallized from MeOH/EtOAc to yield 32% for **1**, 62% for **2** and 75% for **3**

of yellow powders.

Spectral data relative to compound ***1*** ^{1}H NMR (DMSO-d_6): δ ppm 3.07 (s, 6H), 3.2–3.8 (2H,m), 4.67 (2H, t, $J = 7.5$ Hz), 6.85 (2H, d, $J = 5.0$ Hz), 7.53 (1H,s), 8.03 (2H, d, $J = 5.0$ Hz), 8.32 (2H, d, $J = 6.5$ Hz), 8.8 (2H, d, $J = 7.0$ Hz) 10.93 (1H, s) ^{13}C NMR (DMSO-d_6): δ ppm 12.4, 41.3, 48.2, 52.9, 110.9, 112.7, 125.9, 128.4, 130.2, 139.2, 146.4, 150.8, 155.1, 163.7. HRESIMS *m/z* found 430.1020 (calcd for $C_{32}H_{44}NO_3$ [M]+, 430.1016).

Spectral data relative to compound ***2*** ^{1}H NMR (DMSO-d_6): δ ppm. 1.74 (2H,s), 2.49 (3H,s), 3.07 (6H, s), 3.7 (2H, t, $J = 7.5$ Hz) 4.48 (2H, t, $J = 7.5$ Hz), 6.85 (2H, d, $J = 5.0$ Hz), 7.53 (1H,s), 8.03 (2H, d, $J = 5.0$ Hz), 8.32 (2H, d, $J = 6.5$ Hz), 8.8 (2H, d, $J = 7.0$ Hz), 11.27 (1H,s). ^{13}C NMR (DMSO-d_6): δ (ppm) 12.4, 24.5, 41.3, 48.9, 55.2, 110.9, 112.7, 125.9, 128.4, 130.2, 139.2, 146.4, 150.8, 155.1, 155.3, 163.7. HRESIMS *m/z* found 444.1231 (calcd for $C_{32}H_{44}NO_3$ [M]+, 444.1233).

Spectral data relative to compound ***3*** ^{1}H NMR (DMSO-d_6): δ ppm 1.99 (2H, t, $J = 7.5$ Hz), 2.85 (2H, s,), 1.73 (3H, s) 1.87 (2H, t, $J = 7.5$ Hz), 3.07 (s, 6H), 3.7 (2H, t, $J = 7.5$ Hz) 4.48 (2H, t, $J = 7.5$ Hz), 6.86 (2H, d, $J = 5.0$ Hz), 7.53 (1H,s), 8.03 (2H, d, $J = 5.0$ Hz), 8.33 (2H, d, $J = 6.5$ Hz), 8.79 (2H, d, $J = 7.0$ Hz), 11.25 (1H,s). ^{13}C NMR (DMSO-d_6): δ ppm 12.4, 25.6, 28.0, 34.8, 40.1, 40.2, 40.4, 40.6, 47, 49.1, 58.8, 109.0, 112.6, 119.2, 121.4, 130.1, 141.9, 144.1, 151.4, 153.5, 154.4, 164.8. HRESIMS *m/z* found 458.1338 (calcd for $C_{32}H_{44}NO_3$ [M]+, 458.1336).

2.3. Absorbance and emission characterization of MRs 1, 2 and 3

Absorbance spectra of 10 μM solutions of **1**, **2** and **3** in methanol, octanol, water and PBS were recorded at 25 °C ($\lambda_{max,\ abs} = 423$ nm). Emission spectra of solutions 1 μM of **1**, **2** and **3** were recorded ($\lambda_{ex} = 423$ nm, $\lambda_{em} = 440$–700 nm) in the same experimental conditions. The fluorescence quantum yields (Q) of 1 μM solution of **1**, **2** and **3** were measured in methanol, octanol, chloroform and PBS at 25 °C, on

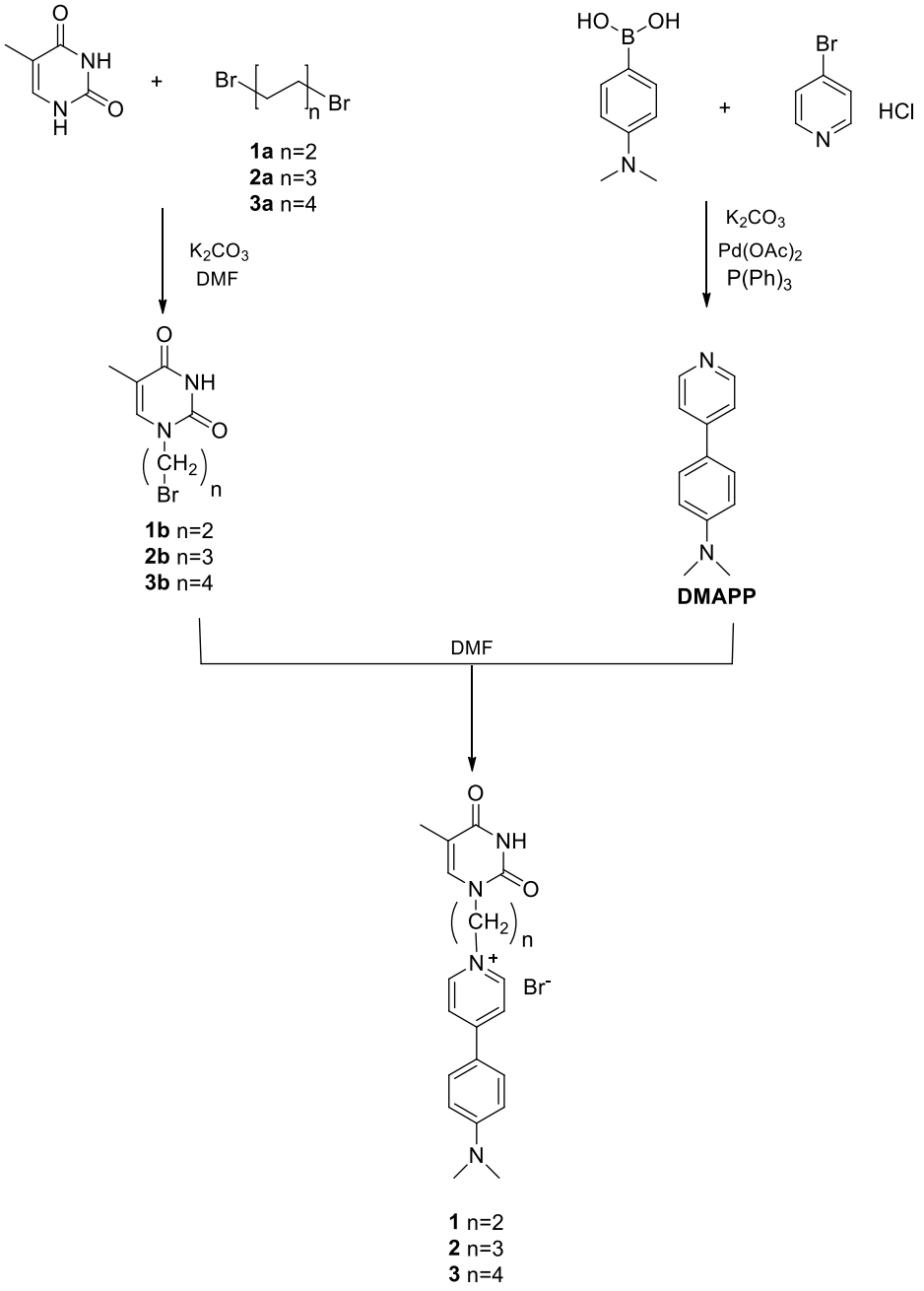

Scheme 1. Synthetic pattern for the preparation of the **1**–**3** derivatives.

solutions with absorbance lower than 0.05 to minimize inner filter effects. Perylene in cyclohexane was used as a reference for quantum yields.[21] Photoluminescence quantum yield (Q) of amphiphile solutions was determined by comparing the wavelength-integrated intensity of an unknown sample to that of a cyclohexane solution of perylene used as a standard. The quantum yield of the unknown sample was calculated according to equation (1):

$$Q = Q_R \frac{I_R}{I} \frac{OD_R}{OD} \frac{n^2}{n_R^2} \quad (1)$$

where I is the integrated intensity, n is the refractive index, and OD is the optical density. The subscript R refers to the reference fluorophore of known Q.

2.4. Binding of compounds 1, 2, 3 with TP

In order to study the interaction of compounds **1**, **2** and **3** with TP enzyme, emission fluorescent spectra (λ_{exc} = 430 nm) were run in the presence of a fixed TP concentration (3 μM) varying the concentration of MR (0.18–1.8 mM). The plot of the maximum fluorescent emission (λ_{max} = 517 nm) *vs* TP enzyme concentration gave the corresponding binding curve and the binding constant (K_d) was determined from curve fitting.

3. Results and discussion

3.1. Synthesis of the fluorescent molecular MRs 1–3

MRs **1, 2** and **3** were prepared according to Scheme 1.

Compounds **1**–**3** were prepared by alkylating 4-[4-(1-dimethylamino)phenyl]-pyridine, DMAPP, with synthetic products **1b**, **2b** and **3b** obtained by reacting the corresponding αω-dibromoalkanes (**1a**, **2a** and **3a**) with 4 equivalents of thymine in the presence of a stoichiometric amount of K_2CO_3 according to a procedure reported in literature.[22] The yield of both reactions is higher as the length of the alkyl spacer increases. Probably the short alkyl spacer, that characterizes compounds **1**, involves steric hindrance in the nucleophilic substitutions. Molar ratios were optimized in order to reduce the amount of dialkylated product. DMAPP was prepared as previously reported[23] by a Suzuki cross coupling of 4-bromopyridine with 4-(dimethylamino)phenylboronic acid.

3.2. Characterization of the fluorescent molecular MRs 1–3

All the photophysical features of the novel amphiphilic fluorescent MRs were investigated in different solvents. Absorbance and emission spectra were recorded in solvent with different polarity and viscosity, *i.e.* PBS and methanol, characterized by high polarity and low viscosity, octanol, characterized by high viscosity and low polarity, and chloroform that features a low viscosity and the lowest polarity.[24,25] **1**–**3** fluorescent MRs are organic cationic dyes that display solvatochromic photophysical properties. Their absorption maxima are blue-shifted in polar media, ranging from 423 nm in PBS or alcohols to 436 nm in chloroform (Table 1). As expected the presence and the length of the alkyl chain do not significantly influence the absorption properties of the fluorophore in all the solvents investigated. In Figure 2 the absorption and emission spectra of compound **3** in different solvents are reported as an example.

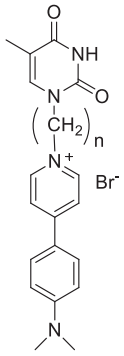

1 n=2
2 n=3
3 n=4

Chart 2. Molecular structure of fluorescent molecular sensors **1**, **2**, **3**.

The red-shift and the lower intensity in fluorescence emission observed in octanol with respect to chloroform is probably due to its higher polarity (μ = 1.76 D and μ = 1.04D for octanol and chloroform, respectively).[23]

On the other hand, the emission of **1**–**3** is quenched in polar and scarcely viscous solvents (Table 1). These results are in good agreement with those reported in the case of MRs containing the *p*–(dimethy1amino) group.[26]

As a whole, absorbance and emission spectroscopies indicate that the three fluorescent MRs exhibit similar photophysical behavior, including high sensitivity to the medium polarity as shown by their ability to access the non-fluorescent TICT state and, hence, to reduce their emission signal.

3.3. Fluorescence of the MRs upon binding with TP

The ability of the MRs **1**–**3** to give a flurescent signal due to TICT process induced by the binding with TP was assessed by fluorescence experiments. A fluorescent signal switched on in the presence of TP in the case of the MR **1** (Figure 3a) whereas the presence of the enzyme did not induce any fluorescent signal in the case of MRs **2** and **3,** as shown in Figure 3b in the case of compuond **3** reported as example.

In the case of **1** the emission induced by the presence of TP is centered at ~ 517 nm, value of wavelength very similar to the value observed in the case of the emission spectrum of the MR in octanol. On the other hand, in the case of **2** and **3** no fluorescence is observed in the presence of TP. This finding suggests either that no binding occurs or that upon the binding of the enzyme the MR is located in a different environment with respect to **1** characterized by different polarity and/or viscosity. Considering that in the case of **2** and **3** the difference with **1** is one or two methylenes in the alkyl spacer, respectively, is unlikely that these molecules can fold in such a way that their binding to the active site of TP is hindered. It is more reliable to hypothesize that, despite the interaction with the enzyme, the probe is not properly geometrically confined; as a consequence, its twisting is not limited, or at least not enough, to block the molecules in a configuration that results in a turn-on emission. At this purpose, we decided to carry out molecular dynamics simulations of the complexes of **1**, **2** or **3** with TP in aqueous solution in thermal conditions which will be reported in a fortcoming study. Preliminary results, reported in detail in the Supplementary Information, show a markedly different behaviour of **1** with respect to **2** and **3.** More precisely, only the former, along the whole simulation time, appears as stably confined within the initial configuration[27] hence qualitatively explaining, although not fully elucidating, the different

Table 1
Photochemical properties of fluorescent MRs **1**, **2** and **3**.

MRs	SOLVENTS METHANOL ε (λ = 425) $cm^{-1}M^{-1}$	Q	PBS ε (λ = 423) $cm^{-1}M^{-1}$	Q	OCTANOL ε (λ = 423) $cm^{-1}M^{-1}$	Q	CHLOROFORM ε (λ = 436) $cm^{-1}M^{-1}$	Q
1	31,000	-	25,000	-	28,000	0.63	37,000	0.87
2	35,000	-	26,000	-	29,000	0.62	38,500	0.95
3	32,000	-	23,000	-	29,900	0.69	38,600	0.95

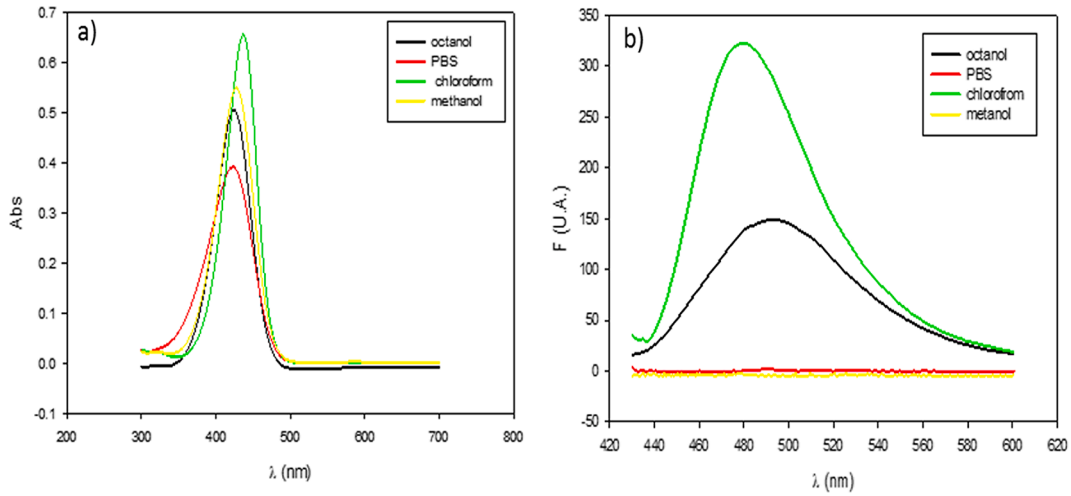

Fig. 2. Absorbance and emission spectra of **3** in different solvents.

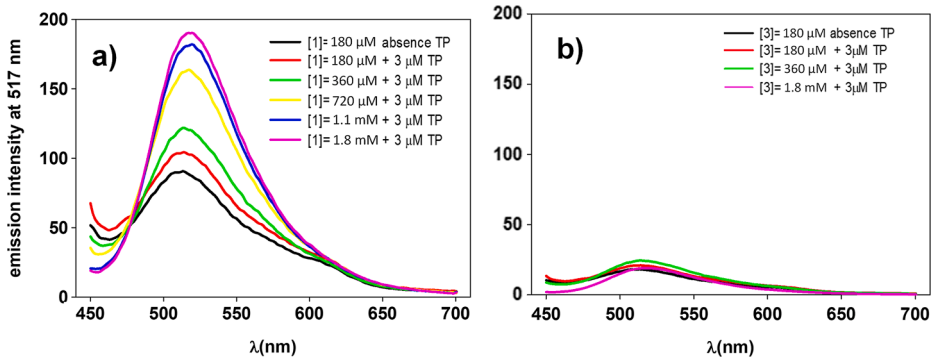

Fig. 3. (a) Fluorescent spectra of samples containing different amounts of compound **1** (left) and **3** (right) in the presence and in the absence (black trace) of 3 μM TP.

spectroscopic behaviour in the presence of the protein.

To evaluate the K_d of the binding of the MR with the target enzyme the intensity of the emission of increasing amounts of the MR was investigated in the presence of a given amount of TP. The plot of the intensity of the maximum at 517 nm *versus* the concentration of **1** (Figure 4) shows that the intensity of the fluorescent signal increases as a function of the amount of **1** up to a threshold value that corresponds to the saturation of the binding site of the enzyme.

The obtained K_d value, 200 μM, is in good agreement with the data reported in the literature[28] concerning the binding of thymine to TP.

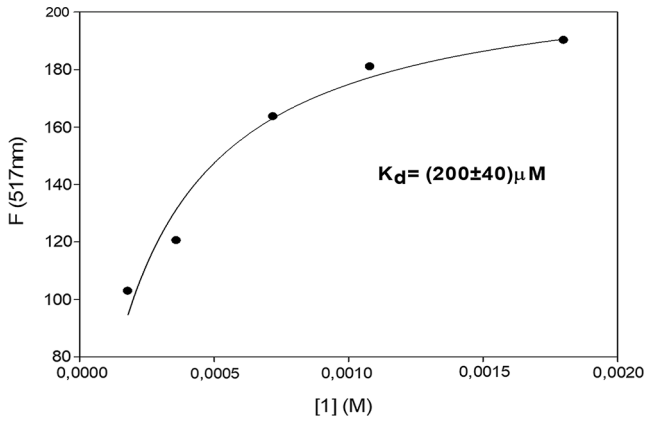

Fig. 4. Plot of the intensity of fluorescence band of **1** in the presence of 3 μM TP, at 517 nm, as a function of concentration of **1**.

This result indicates that the functionalization of thymine at the N^3 position does not affect its ability to interact with the target enzyme (*i.e.* functionalization does not hamper the access of thymine to the binding site of TP). Therefore is reasonable to assume that also **2** and **3**, though featuring a longer alkyl spacer, bind to the active site of TP without being embedded in a chemical microenvironment that induces the occurrence of a fluorescent signal.

4. Conclusions

Three new fluorescent amphiphilic MRs **1**, **2** and **3**, differing in the length of the alkyl spacer joining the receptor unit, a thymine moiety, and a MR as fluorophore were synthesized and characterized. Their potentiality as extrinsic molecular fluorescent sensors to detect the target enzyme TP was investigated. The study of the interaction of **1**–**3** with TP revealed that only compound **1** is able to exhibit a "turn-on" fluorescent signal upon the binding with the enzyme through the elimination of a non-radiative quenching in the less polar environment of the enzyme binding site. On the other hand, the other two MR **2** and **3** does not give any fluorescent signal in the presence of the target enzyme. As a consequence, the relaxation from the excited state proceeds mainly via the nonradiative TICT pathway. The finding that one of the newly synthesized MRs is able to detect the presence of TP enlarges the prospective of exploitation of MRs in the design of molecular sensors and constitutes a proof of principle that could be extended to the fast and easy detection of biological markers.

Declaration of Competing Interest

The authors declared that there is no conflict of interest.

Acknowledgements

The authors thank Prof. Massimiliano Aschi for his support in theoretical calculations.

Appendix A. Supplementary data

Supplementary data to this article can be found online at https://doi.org/10.1016/j.bmc.2020.115881.

References

1 Saif MW, Choma A, Salamone SJ, Chu E. Pharmacokinetically Guided Dose Adjustment of 5-fluorouracil: a Rational Approach to Improving Therapeutic Outcomes. *J Natl Cancer Inst*. 2009;101:1543–1552.
2 Alvarez P, Marchal JA, Boulaiz H, et al. 5-Fluorouracil derivatives: a patent review. *Expert Opin Ther Patents*. 2012;22(2):107–123.
3 Elamin, Y. Y.; Rafee, S.; Osman, N.; O'Byrne, K. J.; Gately, K. Thymidine Phosphorylase in Cancer; Enemy or Friend? Cancer Microenviron. 2016, 9(1), 33–43.
4 Shimada S, Sano D, Hyakusoku H, et al. Dihydropyrimidine Dehydrogenase Overexpression Correlates With Potential Resistance to 5-fluorouracil-based Treatment in Head and Neck Squamous Cell Carcinoma. *Transl Cancer Res*. 2018;7(2):411–419.
5 Morawska K, Goirand F, Marceau L, et al. 5-FU Therapeutic Drug Monitoring as a Valuable Option to Reduce Toxicity in Patients With Gastrointestinal Cancer. *Oncotarget*. 2018;9:11559–11571.
6 Saif MW, Syrigos K, Mehra R, Mattison LK, Diasio RB. Dihydropyrimidine Dehydrogenase Deficiency (DPD) in GI Malignancies: Experience of 4-Years. *Pak J Med Sci Q*. 2007;23(6):832–839.
7 Lee JJ, Beumer JH, Chu E. Therapeutic Drug Monitoring of 5-fluorouracil. *Cancer Chemother Pharmacol*. 2016;78(3):447–464.
8 Macaire P, Morawska K, Vincent J, et al. Therapeutic Drug Monitoring as a Tool to Optimize 5-FU–based Chemotherapy in Gastrointestinal Cancer Patients Older Than 75 Years. *Eur J Cancer*. 2019;111:116–125.
9 Du J, Hu M, Fan J, Peng X. Fluorescent Chemodosimeters Using "Mild" Chemical Events for the Detection of Small Anions and Cations in Biological and Environmental Media *Chem. Soc. Rev.* 2012;41:4511–4535.
10 Liu SY, He YB, Qing GY, Xu KX. Fluorescent Sensors for Amino Acid Anions Based on Calix[4]arenes Bearing Two Dansyl Groups. *Tetrahedron Asymmetry*. 2005;16:1527–1534.
11 Meng LZ, Mei GX, He YB, Zeng ZY. Synthesis and Anion Recognition Properties of Two Novel Tetraamide Calix[4](aza)crowns for Optical Anion Sensor. *Acta Chim Sinica*. 2005;63:416–420.
12 Lee JY, Kim SK, Jung JH, Kim JS. Bifunctional Fluorescent Calix[4]arene Chemosensor for Both a Cation and an Anion. *J Org Chem*. 2005;70:1463–1466.
13 Kashyap B, Dutta K, Das DK, Phukan P. Structurally Simple Ferrocene Derivatives for Selective Cadmium Sensing. *J. Fluoresc*. 2014;24(3):975–981.
14 Petaccia M, Giansanti L, Leonelli F, La Bella A, Gradella Villalva D, Mancini G. Fluorescent Lipid Based Sensor for the Detection of Thymidine Phosphorylase as Tumor Biomarker. *Sens. Actuators B Chem.* 2017;245:213–220.
15 Rettig W, Strehmel B, Majenz W. The Excited States of Stilbene and Stilbenoid Donor–acceptor Dye Systems. A theoretical study. *Chem. Phys.* 1993;173(3):525–537.
16 Strehmel B, Seifert H, Rettig W. Photophysical Properties of Fluorescence Probes. A Model of Multiple Fluorescence for Stilbazolium Dyes Studied by Global Analysis and Quantum Chemical Calculations. *J Phys Chem B*. 1997;101(12):2232–2243.
17 Cogan S, Zilberg S, Haas Y. The Electronic Origin of the Dual Fluorescence in Donor−acceptor Substituted Benzene Derivatives. *J Am Chem Soc*. 2006;128(10):3335–3345.
18 Georgieva I, Aquino AJA, Plasser F, Trendafilova N, Köhn A, Lischka H. Intramolecular Charge-transfer Excited-state Processes in 4-(*N*, N-Dimethylamino) benzonitrile: the Role of Twisting and the πσ* State. *Phys. Chem. A*. 2015;119(24):6232–6243.
19 Zhong C. The Driving Forces for Twisted or Planar Intramolecular Charge Transfer. *PCCP*. 2015;17:9248–9257.
20 Wilson JN, Ladefoged LK, Babinchak WM, Schiøtt B. Binding-Induced Fluorescence of Serotonin Transporter Ligands: A Spectroscopic and Structural Study of 4-(4–(Dimethylamino)phenyl)-1-methylpyridinium (APP+) and APP+ Analogues. *ACS Chem Neurosci*. 2014;5:296–304.
21 Zbigniew R, Rotkiewicz K, Wolfgang R. Structural Changes Accompanying Intramolecular Electron Transfer: Focus on Twisted Intramolecular Charge-transfer States and Structures. *Chem Rev*. 2003;103(10):3899–4032.
22 Lan T, Chen X, Liu Z, Mao Z. A Novel Facile Synthesis Method of *N*-Vinylpyrroles. *J. Heteroc. Chem.* 2013;50(5):1094–1098.
23 Karpowicz RJ, Dunn M, Sulzer D, Sames D. APP+, a Fluorescent Analogue of the Neurotoxin MPP+, is a Marker of Catecholamine Neurons in Brain Tissue, but Not a Fluorescent False Neurotransmitter. *ACS Chem Neurosci*. 2013;4:858–869.
24 Merck Index 85th ed. CRC Press: Boca Raton, FL, CRC Handbook of Chemistry and Physics 2004-2005.
25 Casagrande G, Bianchi E, Costantino ML. Computational Model of Red Cell Flow in Microchannels for Probing Molecules Encapsulation. *Int. J. art. Organs*. 2014;37:602–651.
26 Maskevich AA, Kurhuzenkau S, Yu A, Lickevich A. Fluorescence Spectral Analysis of Thioflavin t–γ-cyclodextrin Interaction. *J. Appl. Spect.* 2013;80:36–42.
27 Petaccia M, Gentili P, Besker N, et al. Kinetics and mechanistic study of competitive inhibition of thymidinephosphorylase by 5-fluoruracil derivatives. *Coll Surf B*. 2016;140:121–127.
28 Panova NG, Alexeev CS, Kuzmichov AS, et al. Substrate Specificity of *Escherichia Coli* Thymidine Phosphorylase. *Biochem (Mosc)*. 2007;72:21–28.